Experimental study on silver coated twisted and coiled polymer muscles, 1-Ply and 2-Ply

Farzad Karami
Humanoid, Biorobotics and Smart Systems (HBS) Laboratory, Department of Mechanical Engineering, The University of Texas at Dallas, Richardson, Texas - 75080, USA.
farzad.karami@utdallas.edu

Lianjun Wu[1]
Humanoid, Biorobotics and Smart Systems (HBS) Laboratory, Department of Mechanical Engineering, The University of Texas at Dallas, Richardson, Texas - 75080, USA.
Wulianjun51@gmail.com

Yonas Tadesse
Humanoid, Biorobotics and Smart Systems (HBS) Laboratory, Department of Mechanical Engineering, The University of Texas at Dallas, Richardson, Texas - 75080, USA.
yonas.tadesse@utdallas.edu

Abstract

Twisted and coiled polymer (TCP) muscles are thermal actuators that generate linear motion as a result of heating. They are finding applications in robotics and biomedical devices due to imperative benefits such as low cost and lightweight. Developing a model for expressing the displacement and force as a function of the inputs (voltage and current) is a current research topic. For identifying the behavior of the TCP muscles in response to the input electrical energy and applied load, one needs a significant number of experimental data at different temperature and load levels. The information gathered from these tests is essential for development, validation, and calibration of any mathematical model. In this work, we report extensive experimental results on silver-coated nylon that are twisted and coiled (TCP_{Ag}) focusing on isotonic tests on 1-ply and 2-ply TCP muscle structures. The electrical input signals, i.e. current and voltage, and the outputs, displacement and the temperature during cyclic tests for several current and load magnitudes are depicted along with deduced results. Temperature and axial load are found to have significant effects on the displacement of these actuators, as it is a thermo-mechanical system. We also conducted a series of simulations using theoretical models in order to correlate the experimental results with the model outcomes.

Keywords: TCP muscle, characterization, soft actuator, modeling, artificial muscle, model calibration, model verification.

[1] Current affiliation: Department of Manufacturing Engineering, Georgia Southern University, Statesboro, Georgia -30458, USA. Email: lwu@georgiasouthern.edu.

1. Introduction

Artificial muscles or actuators are structures that are designed to achieve or mimic the performance of biological muscles. There has been a continuous endeavor among researchers for finding a suitable replacement for the natural muscles to be used in biomimetic systems. Ionic polymer-metal composites, shape memory alloys, and shape memory polymers are among the proposed methods for actuation [1]. By developing new types of smart materials, new opportunities for fabricating device and systems are made possible. The landmark for this achievement was a paper by Haines et al. introducing a twisted coiled polymeric actuator that could show a significant contraction in response to heating [2]. The result is a lightweight, low cost, and high force actuator with several potential applications in the robotics and bioengineering fields. Investigating the behavior of these actuators is the main focus of this work.

Twisted and coiled polymer (TCP) actuator, which is generally categorized as a type of artificial muscles, is a linear actuator that can provide a significant contraction in its length under a mechanical load when subjected to thermal stimuli. The physical phenomenon behind the mechanism of this muscle is the anisotropic physical property of the highly oriented polymers such as nylon and polyethylene. The anisotropic mechanical properties are the result of the oriented structure, opposing to the isotropic properties which are attributed to the random distribution of the molecular orientation throughout the material. In Figure 1, different possible structures of the polymer chains inside a thread are shown. From (a) to (c), the anisotropicity grows as the polymer chains becoming more oriented toward a certain direction.

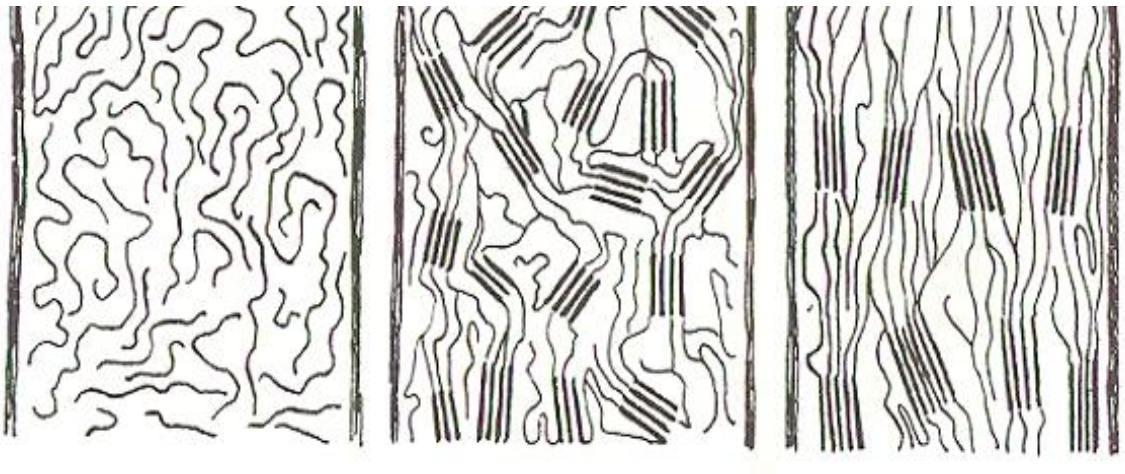

(a) (b) (c)

Figure 1 Schematic diagram of a typical polymer (a) Non-orientated non-crystalline fiber polymer system; (b) Non-orientated but sections ordered fiber polymer system; (c) orientated and crystalline fiber polymer system[3].

Due to a difference in the radial and longitudinal coefficients of thermal expansion (CTE), the twisted string stretches in its longitudinal direction, unwinds and a significant rotation is generated [4-6]. The coiled structure of the actuator converts the rotational untwisting motion of the fibers into the linear contraction. It is the same mechanism here as it is for metallic helical springs except that a metallic wire, due to its isotropic CTE, does not twist around itself by a rise in its temperature. Figure 2 shows a metallic spring and a TCP actuator in order to indicate their behavior in response to heating.

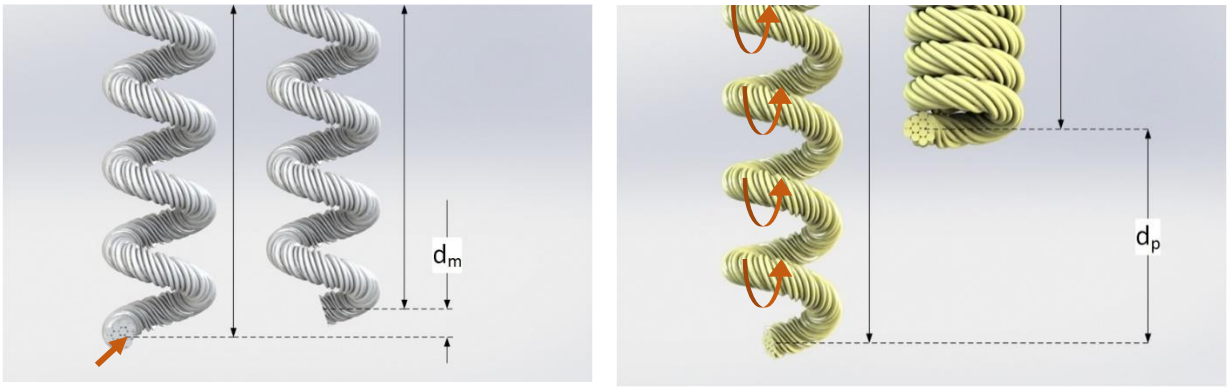

Figure 2: Effect of the heat on the length of a metallic helix (left) and a 1-ply TCP muscle (right). The length change in the metallic spring is due to the isotropic thermal expansion and shows up in the direction of the helix curve. Whereas, 1-ply TCP muscle twists around the central axis and contracts or elongates significantly.

TCP actuators are fabricated by inserting twist into a polymer fiber with a dead weight at the bottom end while being fixed at the other end. By rotating the fiber, the twist is inserted, and the total length of the string starts to decrease. After a certain amount of twist, coil loops start to appear and as more twist inserted, all the straight part of the fiber are eventually converted into a coiled structure. For improving the load capacity of the muscles, several single-ply actuators can be used in parallel. The 2-ply muscle refers to an actuator consisting of two strands wrapped around each other (Figure 3a), consequently have higher stiffness, and higher load carrying capacity than a single one.

The TCP muscles are finding several applications throughout the robotics and bioengineering fields. As an actuator for robotic fingers, Wu et al. proposed a robotic hand powered by a TCP muscle through a tendon-driven mechanism [7], which reduced the weight of the hand comparing to the ones driven by servo motors. In another work, Saharan et al. demonstrated an exoskeleton hand orthosis driven by a set of TCP muscles to help people with an impaired nervous system having assisted hand movements[8]. Using TCP muscles benefits the design in terms of weight and cost, as the overall weight is reported to be less than 100 grams. There are also applications other than the robotic hands such as a reconfigurable robot with tensegrity structure which has light weight and high flexibility, in which TCP muscles served as both support strings as well as actuators [9]. In another work, these actuators are implemented in a biomimetic joint and the muscle-skeleton-joint interaction [10, 11]. Almubarak and Tadesse proposed a method for using TCP muscles embedded in a silicone rubber substrate, mimicking the flexible appendages of animals for biomimicry concepts[12], and other application in making artificial facial expressions on a robotic face and an artificial jaw[13]. Van der Weijde et al. proposed TCP muscles as a displacement sensor by measuring the electrical impedance of the muscles [14]. In another sensor application, Saharan et al. used TCP muscles as a thermostat [15]. Kim et al. presented a new method of TCP muscle actuation with an application in a robotic hand [16]. TCP muscles can also be utilized in energy harvester [17]. Pawlowski et al. presented a method to use TCP muscles embedded in a soft structure serving as a gripper [18].

There are several works dedicated exclusively to experimental studies on TCP muscles. Mendes and Nunes presented an experimental approach for investigating the thermo-mechanical linear actuation behavior of coiled polymer fibers in an isometric test [19] at different temperatures, up to approximately 120 °C. Cherubini et al. also presented thermo-mechanical characterization based on a series of experiments at different temperatures, up to 120 °C, including isothermal and isometric tensile tests [20]. Yue et. al. [21] reported an experimental approach to measure the axial thermal expansion coefficient of the twisted carbon fibers ($-1.1 \times 10^{-6} \sim -4.3 \times 10^{-6}$ °C^{-1}) and Kevlar yarns ($-6.9 \times 10^{-6} \sim -2.4 \times 10^{-6}$ °C^{-1}) in an isotonic test where the maximum temperature is 54°C. Yue et. al. also [22] reported that the normalized effective

Young's modulus (ratio of modulus of pure nylon to the twisted nylon fiber) of twisted and coiled polymer muscles is 0.16 ~ 1.0, which depends on the twist angle and the diameter of twisted strands. Li et al. investigated the effect of annealing stress on the thermal actuation performance of twisted and coiled polymer muscles [23], and reported that the increase of annealing stress can enhance the contraction strain. Swartz et al. investigated the free torsion of a highly twisted polymeric actuator and presented their experimental results for measuring the radial and longitudinal thermal expansion. Then, they validate a model with the experiment [24].

Several models aiming at the prediction of the displacement of the TCP muscles for a given input are developed throughout the literature. A need for high accuracy model that can predict the displacement and force, dictates the necessity of a comprehensive model capable of predicting the displacement based on a given thermal actuation and load. Sharafi et al. showed a model from the polymer science point of view and tried to explain the behavior of the actuator with the concept of a transition between saturated and unsaturated molecular phases [25]. Yang et al. proposed a model for determining the displacement based on the volume fraction of polymeric phases. The model is validated with experimental data up to 80°C [26]. Jafarzadeh et al. conducted a black box analysis to find a model with a satisfactory accuracy and concluded that the first order model is sufficient for force and power relationship assuming constant resistance of the muscles[27, 28]. Arakawa used a similar approach for modeling to control the length of a TCP model under a constant load [29]. Abbas et al. proposed a model for predicting the displacement based on the radial expansion of the fibers [30]. Yip et al. used a first-order model, derived from the heat transfer physics of a TCP muscle, for control of the hand driven by TCP muscles [31]. Zhang proposed a model for explaining the hysteresis behavior of polymer muscles [32]. In another work, they proposed a method based on Preisach models to compensate for the effect of the hysteresis in a control system [33]. In a recent work, Masaya et al. used an energy approach to formulate the behavior of TCP muscles [34]. Their approach is using a gray model, i.e. incorporating parts of the system physics into the model, with a focus on the energy dissipation in the boundaries and neglecting the effect of geometry. Karami and Tadesse proposed a model which incorporates both the temperature and load effect on the displacement into account by using physics of the contributing electro-thermo-mechanical phenomena [35]. Shazed et al. showed a modeling approach by using a single helix model and compare its performance to their experiments [36].

In Figure 3(c) and (d), a magnified view of both types of TCP muscles is shown, illustrating the twisted strands along with the normal views of them in Figure 3 (a) and Figure 3 (b). Although TCP muscles made from sewing thread are easy to actuate via electro-thermal heating, the silver coating that is needed for Joule heating increases the cost of the precursor material compared with its counterpart fishing line. Moreover, our high current pulses tests showed that extremely high power within a short period may lead to the degradation of the muscles life cycles due to flaking of silver from the nylon surface which affects electro-thermal actuation as shown in Figure 3 (e). The bright regions of a 1-ply TCP muscle in Figure 3 (e) indicate those areas where the silver-plated layer flaked from the polymer surface. The high power supplied to the TCP muscle caused the muscle to lose conductivity. As a complementary study, a comparison of the test results and one of the models proposed [35] for predicting the displacement as a function of the temperature are presented. In this analysis, the displacement vs temperature figures are drawn to give a comparison of the model accuracy and the test data and to demonstrate the usability of the experimental data for modeling purpose. It was aimed to conduct the tests for wide intervals of the currents and loads to span all the working space of the actuators and also explore all the phenomena associating with the TCP muscle actuation, particularly finding the limits of this type of actuators. The reported experimental results can be used in any modeling of TCP muscles and also for validation of the already developed models as well as the calibration of the parameters, such as elastic modulus and thermal expansion coefficients. The rest of the paper will

discuss on experimental procedure, results, deduced results and model validation as well as conclusions and future works.

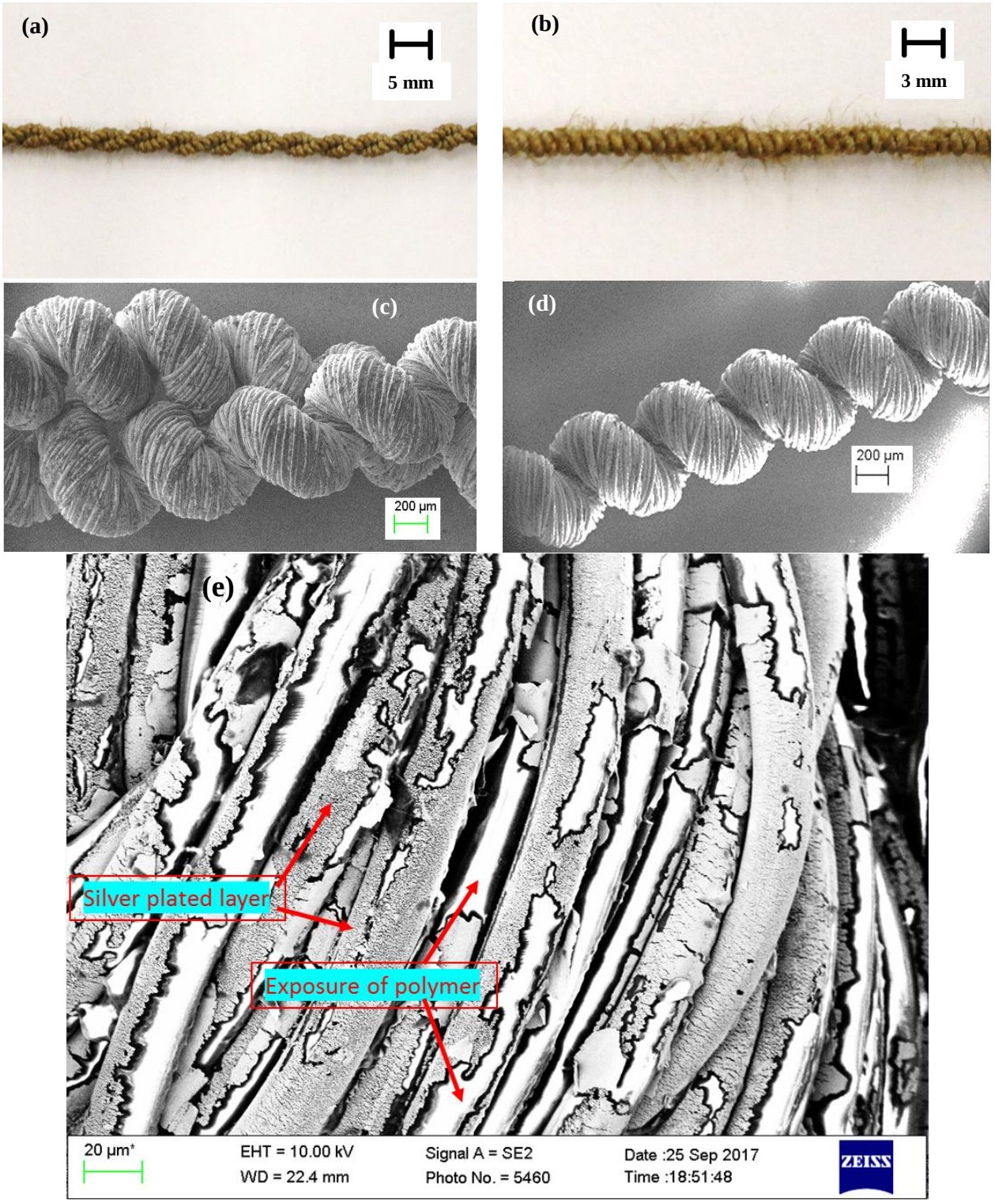

Figure 3: View of 2-ply (a) and 1-ply (b) of TCP muscles. Microscopic view of 2-ply (c) and 1-ply (d) TCP muscles with a 500x magnification factor, (e) SEM image of the defected 1-ply TCP muscle from silver-plated sewing thread.

In this paper, a thorough functional characterization of TCP muscles is presented. Since the TCP muscles possess complaint structure, the final displacement changes by a variation in load. This matter necessitates having an insight into the behavior of the muscles under different loads, as it is a preliminary step in modeling as well as using this actuator.. To do this, a test stand is devised which is able to measure the desired quantities, which are displacement, temperature, force, actuation current, and actuation voltage of TCP muscles. The fundamental concept underlying the exceptional behavior of TCP muscle is a strong relationship between its thermal and mechanical domains of the material. Therefore, the temperature and displacement should be measured as they represent these domains. The current and voltage are measured for quantification of the relationship between the electrical and thermal domains since the Joule heating is the most practical actuation method. The tests are done in a certain range of load and current according to the limits that TCP muscles are actuated. To demonstrate the feasibility of TCP muscles mathematical modeling we used the obtained data for calibration and prediction of the TCP muscles using one of the proposed models. The experiment results showed a good applicability for modeling purpose. In another section, to answer the question for the highest breakage free actuation frequency that we faced in our research, a thermal analysis conducted and the results are presented.

2. Experimental

For comprehensive characterization of TCP muscles, tests were carried out on a test stand in the HBS lab at The University of Texas at Dallas. As it is depicted in Figure 4, the test is done as the muscles are kept horizontally by fixing at one end and being subjected to an axial load by hanging a weight at the other end. The displacement was measured by a Laser displacement sensor (Keyence LK-G152) emitting laser ray to an opaque surface fixed to the TCP muscle end. The temperature is measured by two thermocouples (E-type thermocouples from Omega Engineering Inc.) by making their junctions in touch with the actuator body. The tests are done in a current controlled setup, but the voltage control could be used as they are not fundamentally different. The electrical power was provided by a programmable DC power supply 1687B from BK Precision. An auxiliary electrical circuit was implemented in order to measure the current. The measurements were acquired by NI 9221 and NI 9219 Analog Input Modules plugged in an NI cDAQ-9178 and received in NI LabVIEW through a customized file. The data were read at a 10 Hz rate. The Figure 4 (A) shows a descriptive view of the test stand and Figure 4 (B) is the photo with each component labeled.

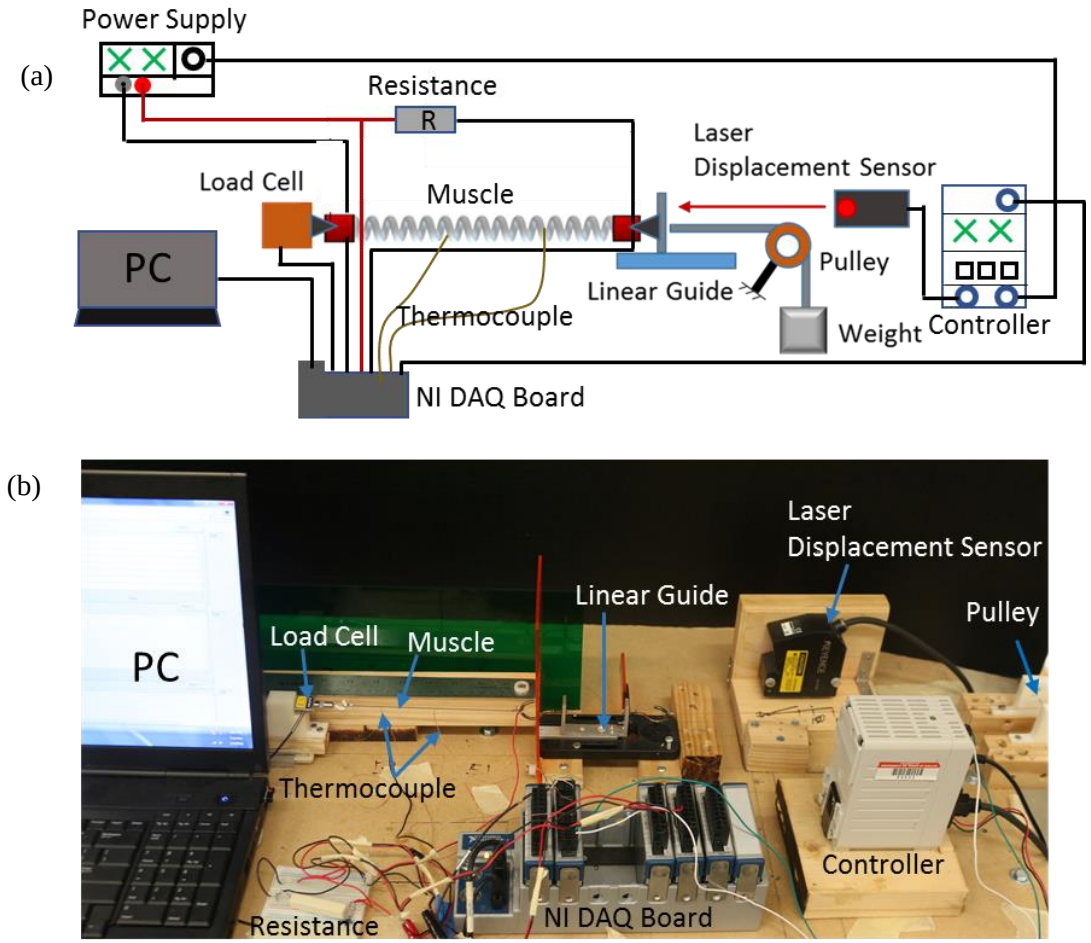

Figure 4: (a) schematic diagram of the experimental setup for characterization of the investigated muscles, and (b) the picture of the laboratory setup

The tests were done in the isotonic mode in which the applied weight was kept constant during the test, hence the axial load throughout the actuator was unchanged. In this way, the effect of the temperature on displacement could be investigated at a certain load. For the 1-ply muscle, the experiment was done at 0.18 A, 0.21 A, 0.24 A, 0.27 A, 0.30 A, and 0.36 A and for the 2-ply at 0.5 A, 0.6 A, and 0.66 A. The weight for the 1-ply muscle was varied at 30, 60, 100, and 200 grams and for the 2-ply it was 50, 100, and 200 grams.

All themuscles were fabricated from the multifilament nylon 6/6 precursor material (PN#26151023534 oz., Shieldex Trading Inc.) coated with silver. The precursor was twisted at a speed of 600 rpm under a 150-gram load until the coils induced by the over twisting formed all along the fiber. Electro-thermal annealing was applied to 1-ply muscle at a current of 0.42A at a duty cycle of 32% under and to 2-ply muscle at a current 0.66A at a duty cycle of 36% under a 300-gram load. The experiments were performed with a heating time of 30 seconds and a cooling time of 45 seconds, a period of total 75 seconds. The specifications of the tested TCP muscles are shown in Table *1*. Such detailed information are not provided in literature regarding TCP fabrication. However, we provide all of them because these parameters determine the overall performance of the muscles. For avoiding the thermal disturbance from the unwanted airflows over the muscles, they were confined in a transparent plastic frame during the test. This box was big enough to act as an ambient air medium.

Table 1: Geometric, physical, and mechanical properties of the TCP muscles used in the experiments.

Parameter	1-ply	2-ply
Precursor Initial Length	500 mm	700 mm
TCP muscle Initial Length	220 mm	270 mm
Initial Precursor Diameter	0.2 mm	0.2 mm
Stiffness at Room Temperature	23 N/m	26 N/m
Fabrication load	150 grams	150 grams
Training load	30 ~200 grams	50 ~ 300grams
Fabrication speed	600 rpm	600 rpm
Annealing Current	0.42 A	0.66 A
Training Current	0.18 ~ 0.36 A	0.50 ~ 0.66 A
Number of Annealing Cycle	6	8
Number of Training Cycle	6	8

3. Experiment Results and Discussions

This section is dedicated to present the test results from the aforementioned experiments. The results are shown in a series of figures including the force, current, voltage, temperature, and displacement time history for four successive actuation and cooling cycles. Figure 5, Figure 6, and Figure 7 show the measurements for the 1-ply muscle and Figure 9, Figure 10, and Figure 11 show the results for 2-ply muscles.

3. 1 Results on 1-ply TCP

In each figure depicted in Figures 5-7 for 1-ply TCP muscles, the first subplot (1st row) shows the force measured by the load cell. Since the dynamic load is minimal due to slow actuation, the slight change in the force, during the actuation, is due to the friction inside the test stand moving parts, the pulley. The second row shows the current, which is the controlled input of the experiments. The third subplot depicts the voltage measured between two terminals of the TCP muscles. Comparing the rising curve of the voltage with the almost constant value of the current implies the changing electrical resistance in the TCP muscles. The change in geometry, as well as the change in the temperature, can attribute to this change. This phenomenon is investigated in [35, 37]. The voltage and current data can be used in finding the suitable electrical resistance of TCP muscle regarding the maximum voltage and current, given that there is a restriction on the power supply size for providing high voltage or current.

The next two subplots (4th and 5th rows) show the displacement and the tensile actuation of the TCP muscles. The first figure of the two shows the absolute displacement measured by the described laser sensor and the second one is the absolute displacement divided by the loaded length of the actuator. As it is expected, higher electrical actuation corresponds to the larger displacement as the temperature rise is more. There is another trend observable in loading under different weights.

The helical geometry underlies the large contraction of the actuator. Transforming this geometry, due to a high load, into a straight piece of the string causes the achievable deflection falls significantly. This observation necessitates considering a limit for the load, other than the material strength limit, in order to have a reasonable actuation.

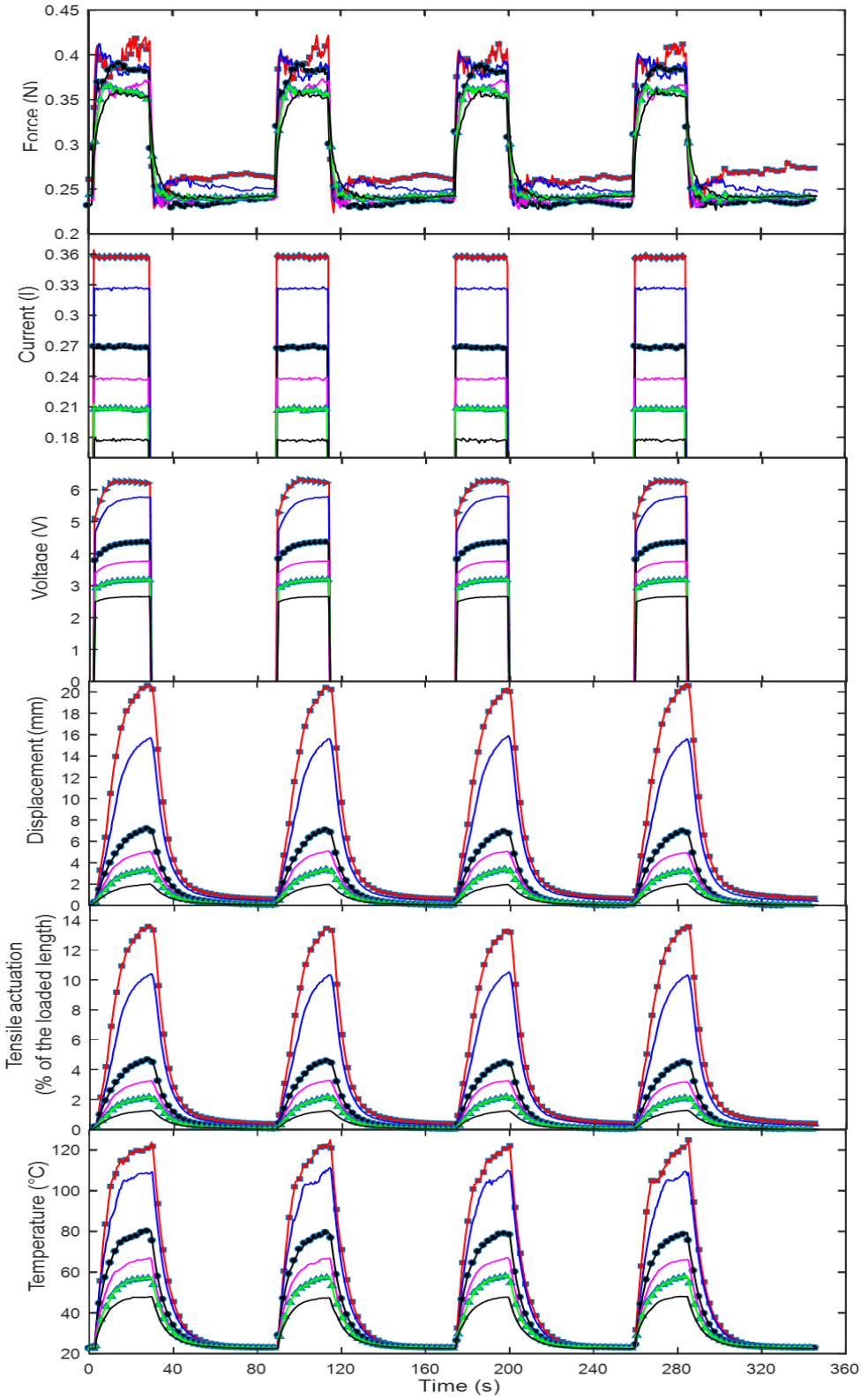

Figure 5: The measured variables of a 1-ply TCP muscle subjected to a 30-gram load in an isotonic test.

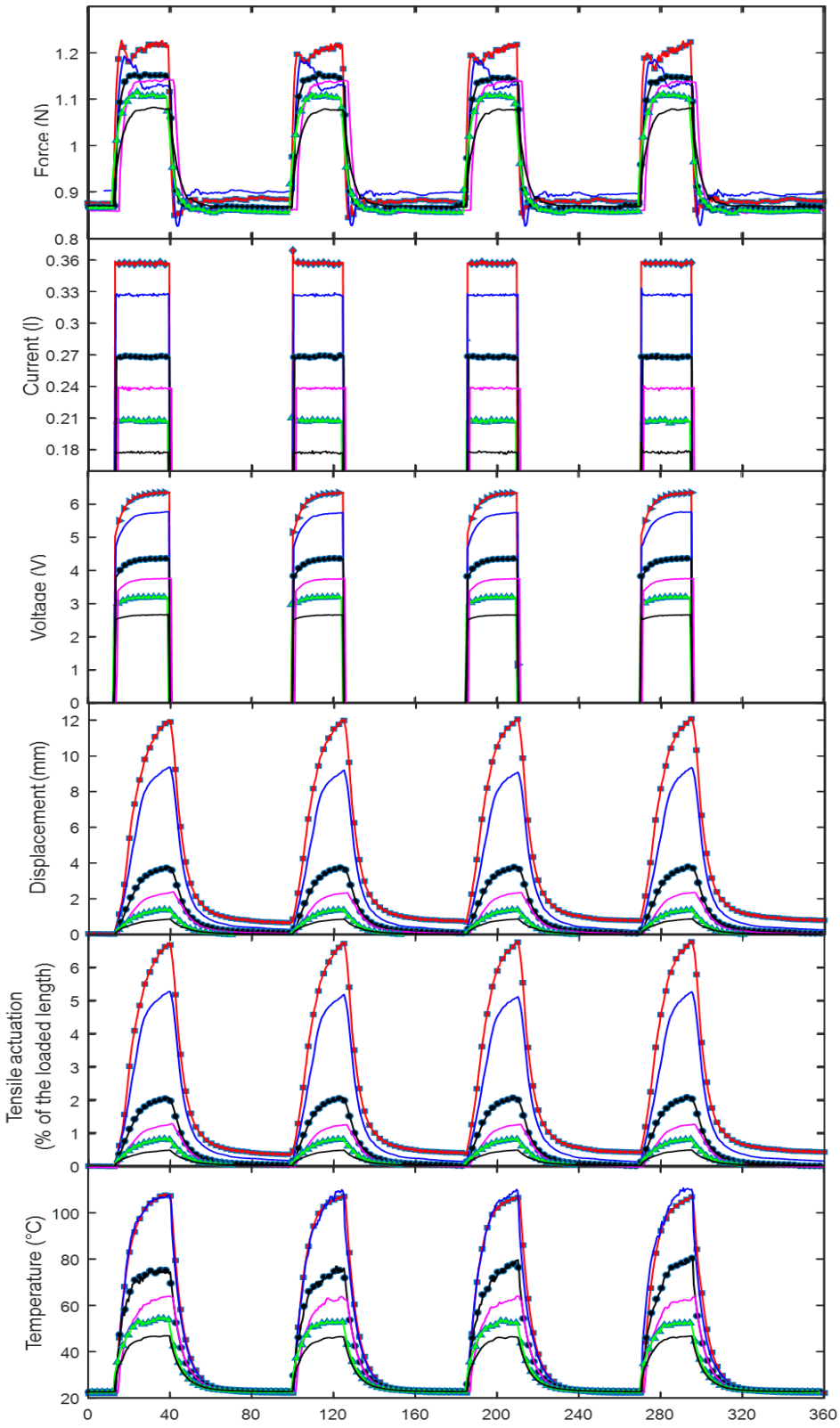

Figure 6 The measured variables of a 1-ply TCP muscle subjected to a 100-gram load in an isotonic test.

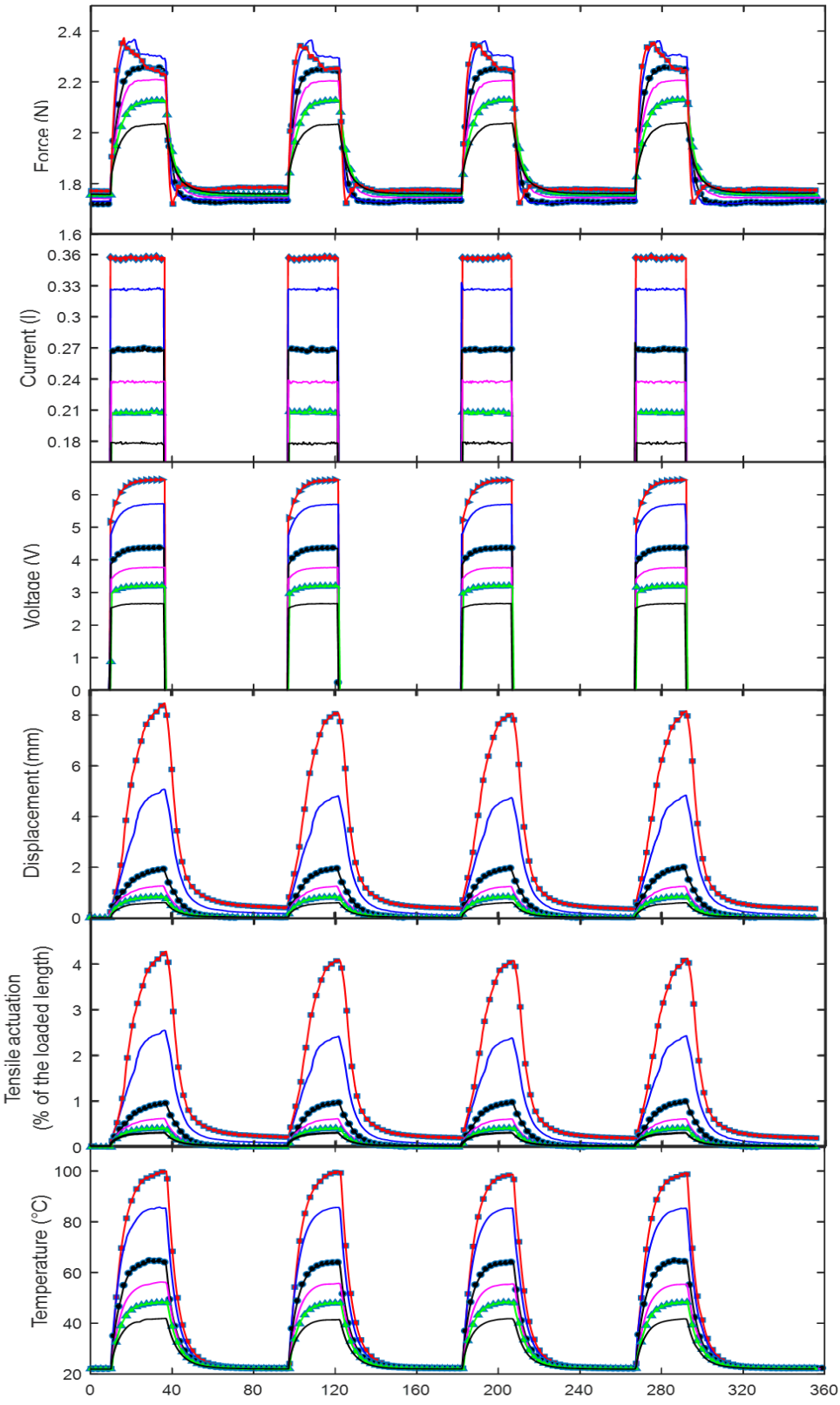

Figure 7: The measured variables of a 1-ply TCP muscle subjected to a 200-gram load in an isotonic test.

Deduced result for 1-Ply TCP

Figure 8 shows experimental results of the twisted and coiled polymer muscle with different current and load conditions, where the symbols designate the experimental results. The effect of load carrying condition on tensile actuation are presented in Figure 8 (a). It is found that (1) with the increase of the carrying load, the tensile stroke decreases significantly at high current input condition, whereas at low current input condition, the effect of carrying load on tensile stroke is minimum; (2) the tensile stroke at light carrying load conditions was more affected by current than that at heavy carrying load conditions. The Figure 8 (b) shows the loaded length of the muscle at different load condition. The loaded length was measured after training and test at each load and current input. One can see that the muscle elongates with the increase of the load. Moreover, at the same load, the current has a slight effect on the length. Figure 8 (c) displays the effect of current on the tensile stroke. It is obvious that the higher current generates larger tensile stroke and the same trend can be found at different load conditions.

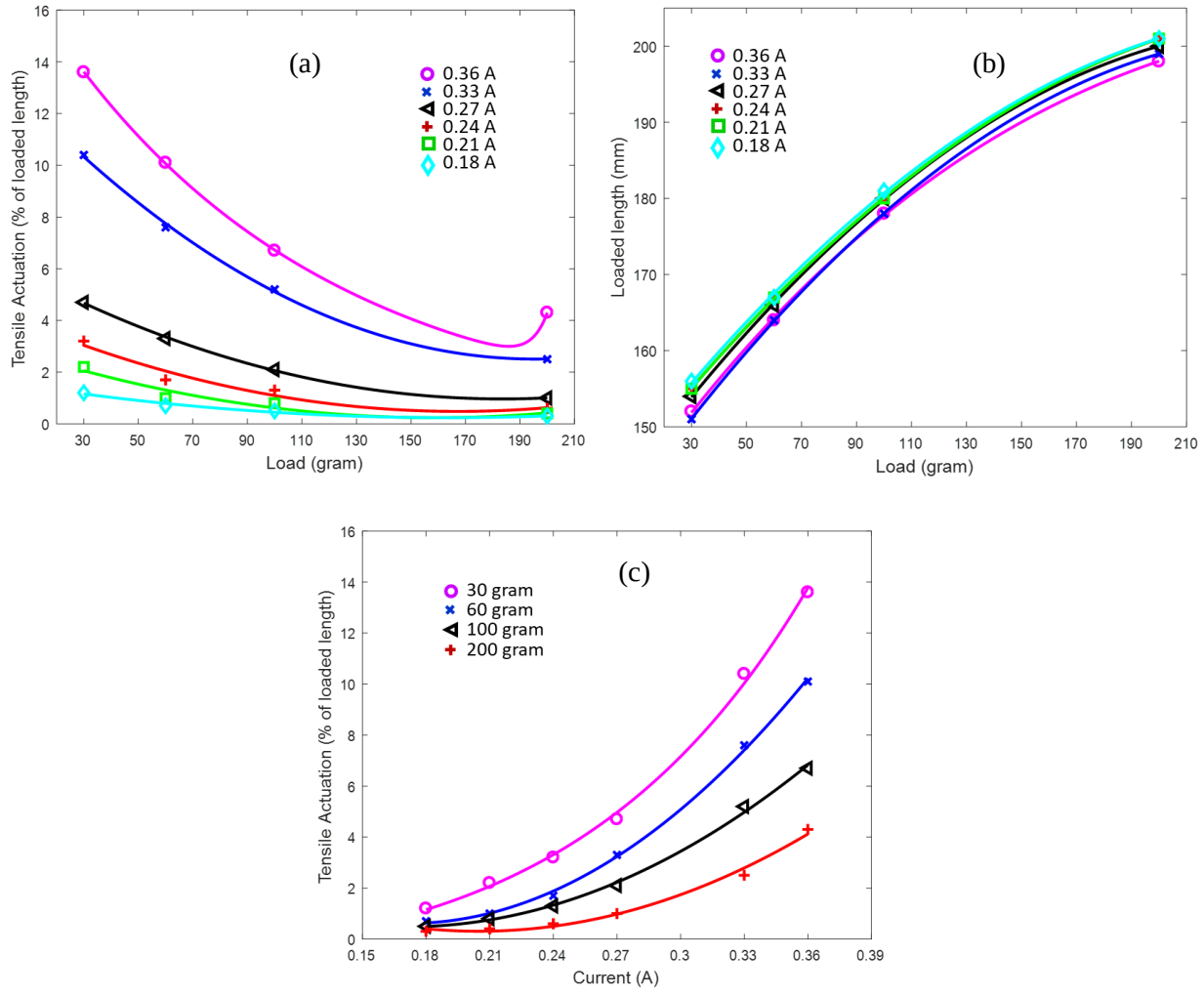

Figure 8: (a) Tensile actuation vs Load, (b) Loaded length vs Load, (c) Tensile actuation Vs current

3.2 Results on 2-Ply TCP

Figure 9, Figure 10 and Figure 11 show the results for 2-ply at different loads (50, 100 and 200g respectively). In all these three figures the temperature (6^{th} row), tensile actuation (5^{th} row), and displacement (4^{th} row) have the same profiles (shapes) except their magnitudes. The other observed phenomenon is at low load and high current actuation, specifically in Figure 9 and Figure 10, where the load is low relative to the stiffness of the actuator. In this case, the heat-induced contraction causes the actuator to fully contract and the coils come into contact with each other. Of course, there would be no more motion and it can be noticed at the flat part of the displacement plot in those two figures. This phenomenon determines a lower limit for the actuator load. The final plot of each figure depicts the temperature measured on the surface of the TCP muscles by using the thermocouple described in earlier section. Fixing of the thermocouple electrodes required a high level of experience and accuracy as the results can be far from the actual values if the electrodes are not firmly secured on the surface. The results show a good correlation between the measured temperature and the actuation current. The temperature measurement has a great importance in modeling the TCP muscles behavior, as it is a driving factor of the change in the dimensions of the actuators. In all the plots, few marker points are shown for illustration of the data points but the actual sampling frequency was 10 Hz and therefore we have several data points that are shown in continuous line.

The stiffness of TCP muscles has a crucial effect on the load capacity. The stiffer they are, the load effect reduces and the overall actuation increases. Therefore, having the stiffness magnitude is an aid for a designer to have a better estimation of the actuator properties and load capacity. In Figure 12, the deflection of the 2-ply versus the applied load is presented. Part (a) is the deduced results from the experiment shown in Fig. 9-11, which is shown for a few data points. This test was done for few applied loads and therefore spline fittings were used to fit the data which increase and decease depending on the load. In another test, a similar 2-ply TCP muscle was characterized at 3 different currents. Figure 12 (b) shows the load dependence of the tensile actuation. The tensile actuation normalized to the loaded muscle length depends mainly on the applied load as the muscle elongates considerably under higher load. The maximum tensile actuation, realized at a constant current 0.66A, was 15 % stroke. The optimal load or the lowest applied load, which resulted in the maximum displacement or tensile actuation of the investigated muscle, was approximately 100 grams, it is obvious that larger tensile actuation was realized at higher current. In the case of constant current 0.60A and 0.55A, the optimal load does not exist within the range from 50 g to 700 g. The main reason is that lower currents could not produce enough heat to actuate the muscle to realize the full amount of actuation. The variation of tensile actuation in (a) and (b) is +/- 2 %, which is consistent with the prior study of such muscles [12].

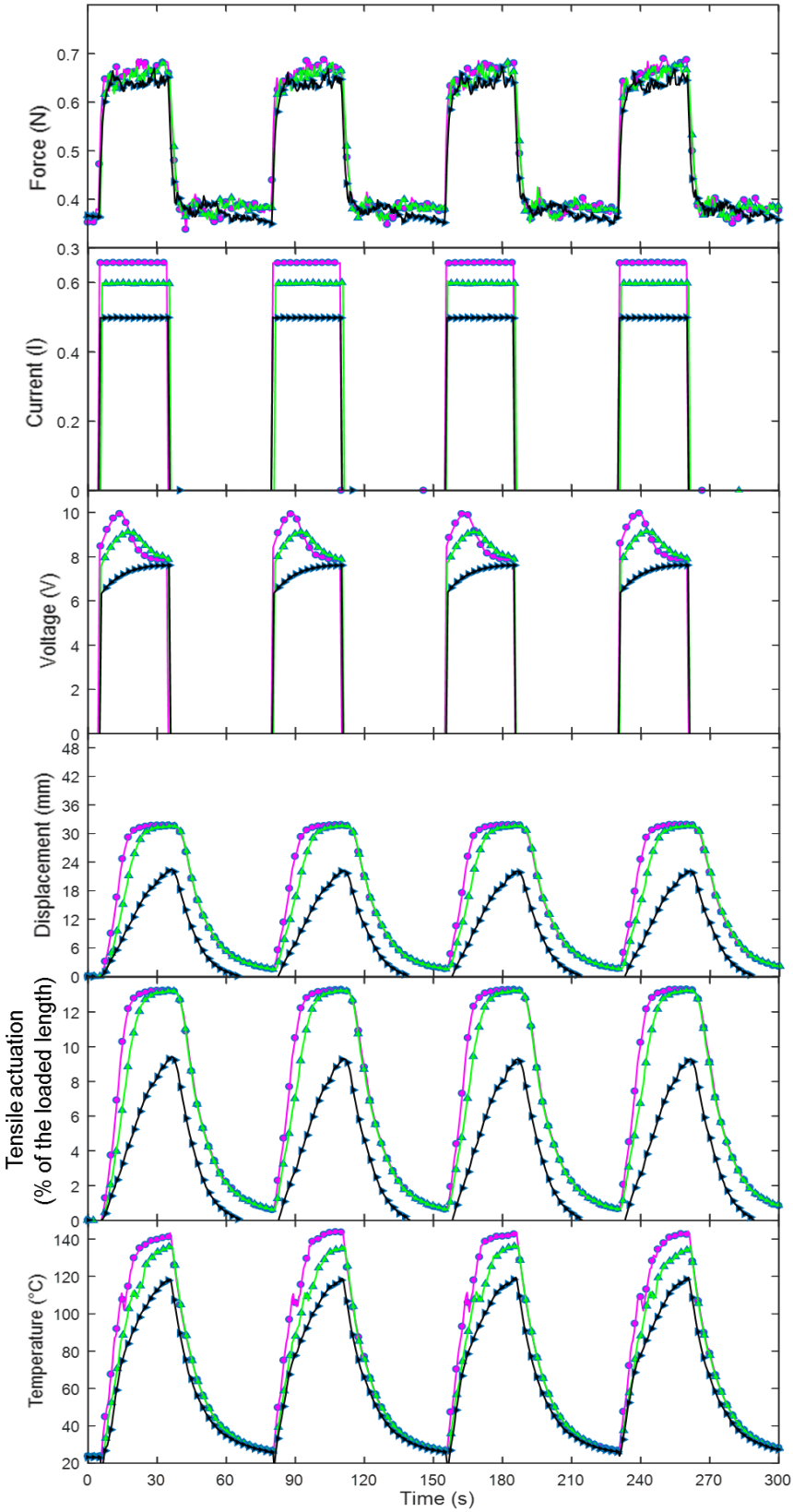

Figure 9: The measured variables of a 2-ply TCP muscle subjected to a 50 grams load in an isotonic test.

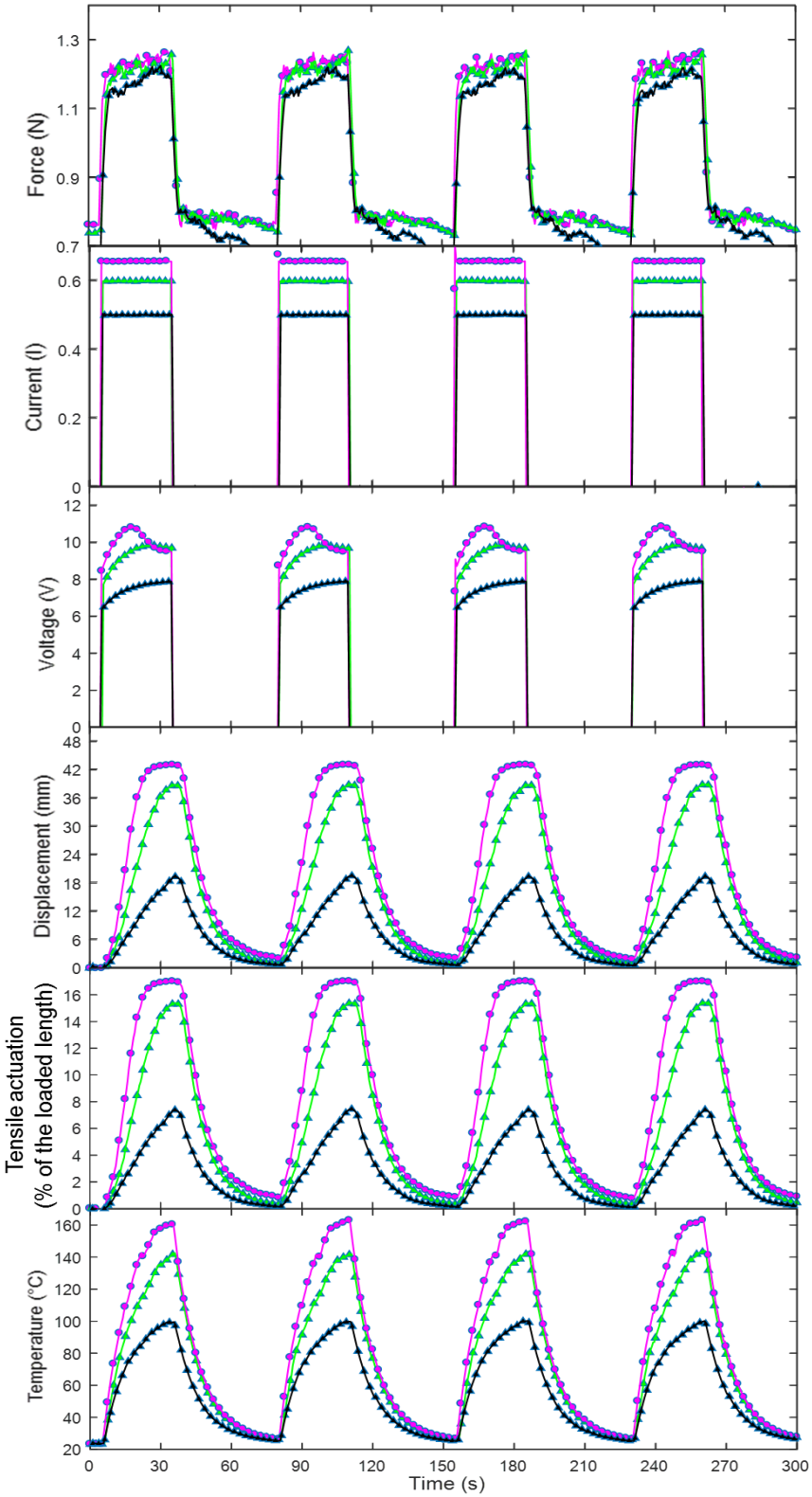

Figure 10: The measured variables of a 2-ply TCP muscle subjected to a 100 grams load in an isotonic test.

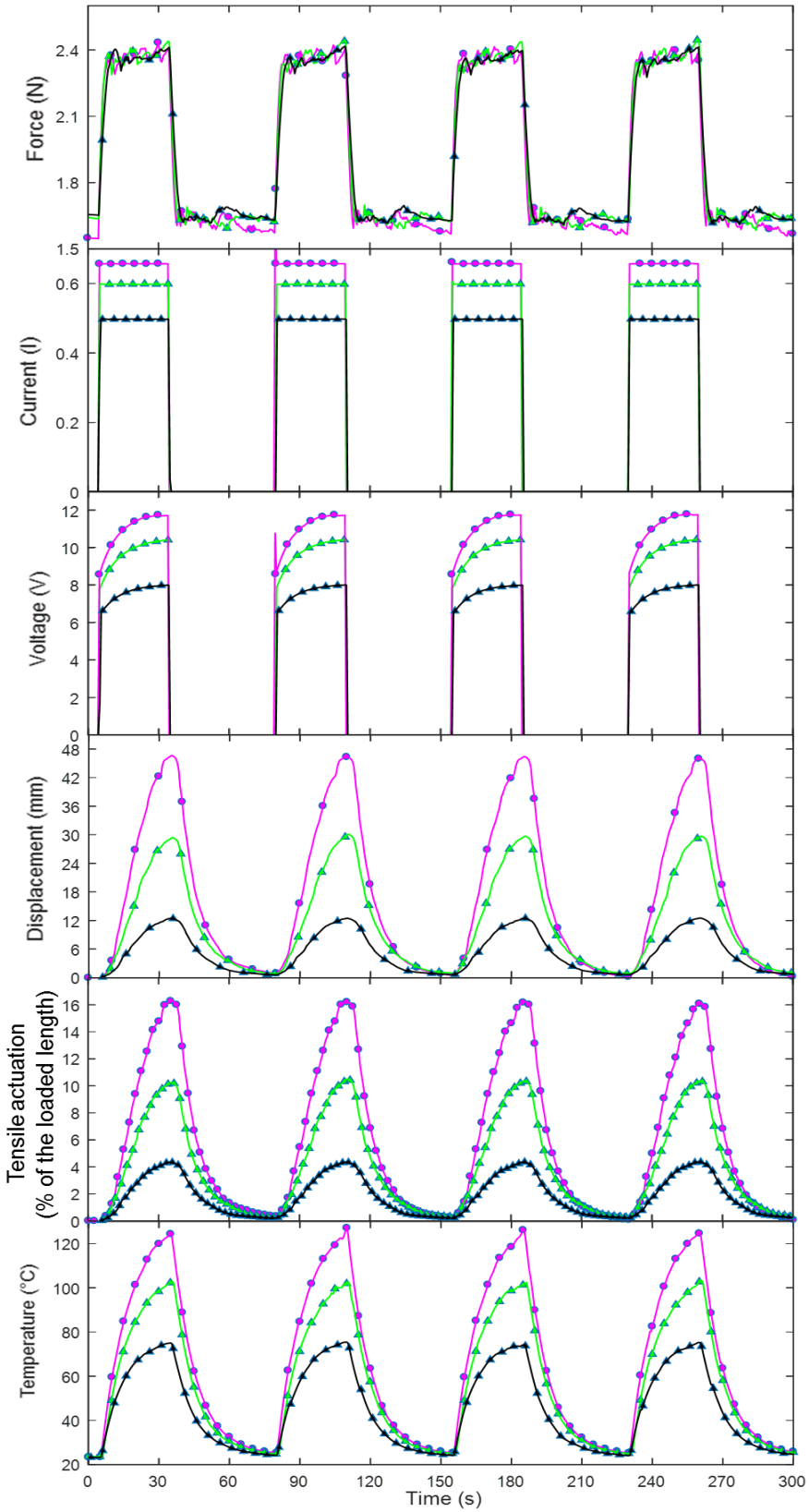

Figure 11: The measured variables of a 2-ply TCP muscle subjected to a 200 grams load in an isotonic test.

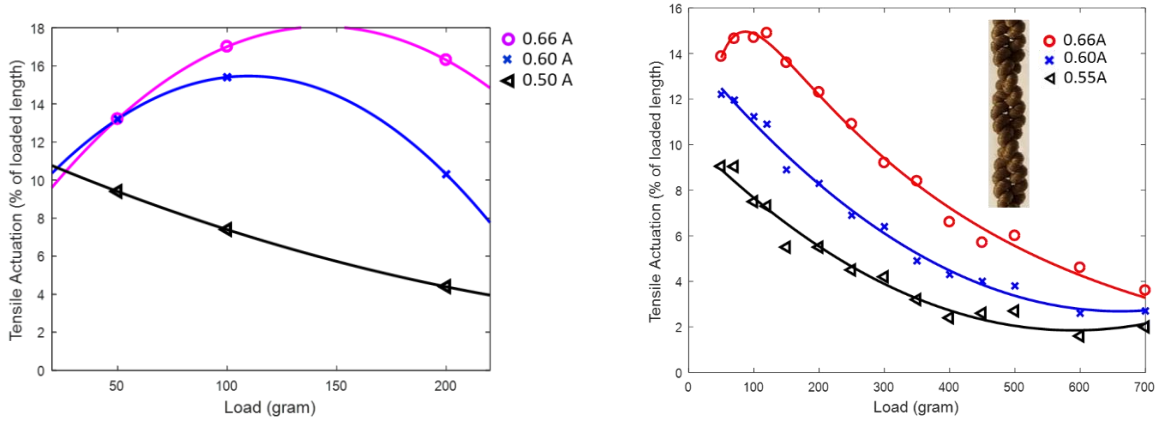

Figure 12: Deduced data for 2-ply TCP muscle Tensile actuation vs Load (a) sample 1 and (b) sample 2.

The summary of the results for a single ply and two ply TCP muscles characteristics is presented in Table 2. This consists of the power, the load, frequency, deflection percentage (actuation stroke) and efficiency, which is a complete performance characteristics of 1-ply and 2-ply muscles. The efficiency of the TCP muscles are calculated as the ratio of the mechanical energy to the input electrical energy. We have shown a 16% actuation at 200g load at 0.66A and 12 V, which is a great performance showing the potential of the actuator for soft robots and other, in addition to the light weight (mass of the actuator, 0.4 gram/meter). However, the efficiency is low, similar to shape memory alloy (SMA). The low efficiency is due to the many factors such as heat dissipation to the environment and friction. It can be improved by forced cooling and studying more materials. The efficiency of TCP muscles are calculated by the following equation:

$$\eta = \frac{E_{friction} + E_{gravity}}{E_{Electrical}} = \frac{F_f d + mgd}{VIt} \tag{1}$$

Where $E_{friction}$ is the friction dissipated energy, $E_{gravity}$ is the gravitational energy stored in the system, m is the mass of the weight, g is the gravitational acceleration, d is the displacement by the TCP muscle, F_f is the friction force, V is the actuation voltage, I is the actuation current and t is the actuation time.

Another issue is the low frequency (10 mHz) reported in this paper, which is a result of the long cooling time needed by the muscle to return to its initial length when we tested in dry state in ambient air. However, this is not the limit of the actuator. Haines et al. showed actuation frequency up to 7 Hz by actuating silver coated TCP in a water environment (wet state) [2]. This requires high power as the actuator is operating in a cooling medium. One should notice that the actuation time cannot be reduced unlimitedly either. The reason is that to achieve a certain amount of the displacement, it is required that the heat distributed throughout the fibers. Similar to other physical phenomenon, it requires a certain amount of time, regardless of how high the temperature is at the boundary. In our case, the heating process is done through releasing the electrical energy in the surface of the fibers and diffuses to the core. Our thermal finite element study shows that large increase in the input electrical energy causes a significant temperature on the surface and much colder temperature in the core. This phenomenon results in the breakage of the fiber without reaching the desired displacement. A fiber model with separate nylon and silver parts was made in the modeling environment and a transient thermal analysis was carried on. In these simulations, the amount of the energy, i.e. the product of the actuation time and electrical power is kept constant. The dimensions of the fibers are acquired from microscope imaging. They were 25 µm and 100 nm for the fiber diameter and coating thickness, respectively. As the actuation time becomes shorter, the temperature gradient grows. It reaches to almost 10^8 as the actuation pulse width falls below 0.01 s. In 0.1s, the obtained temperature gradient is

about 10^5, which causes a temperature difference less than 5°C. According to this result, The thermal behavior of TCP muscles can be estimated by the lumped parameter model in actuation times more than 0.1 sec, which is far less than what is required in the current applications. The results of the FEM analysis, in terms of the temperature distributions over the fiber cross-section, are shown in Figure 13.

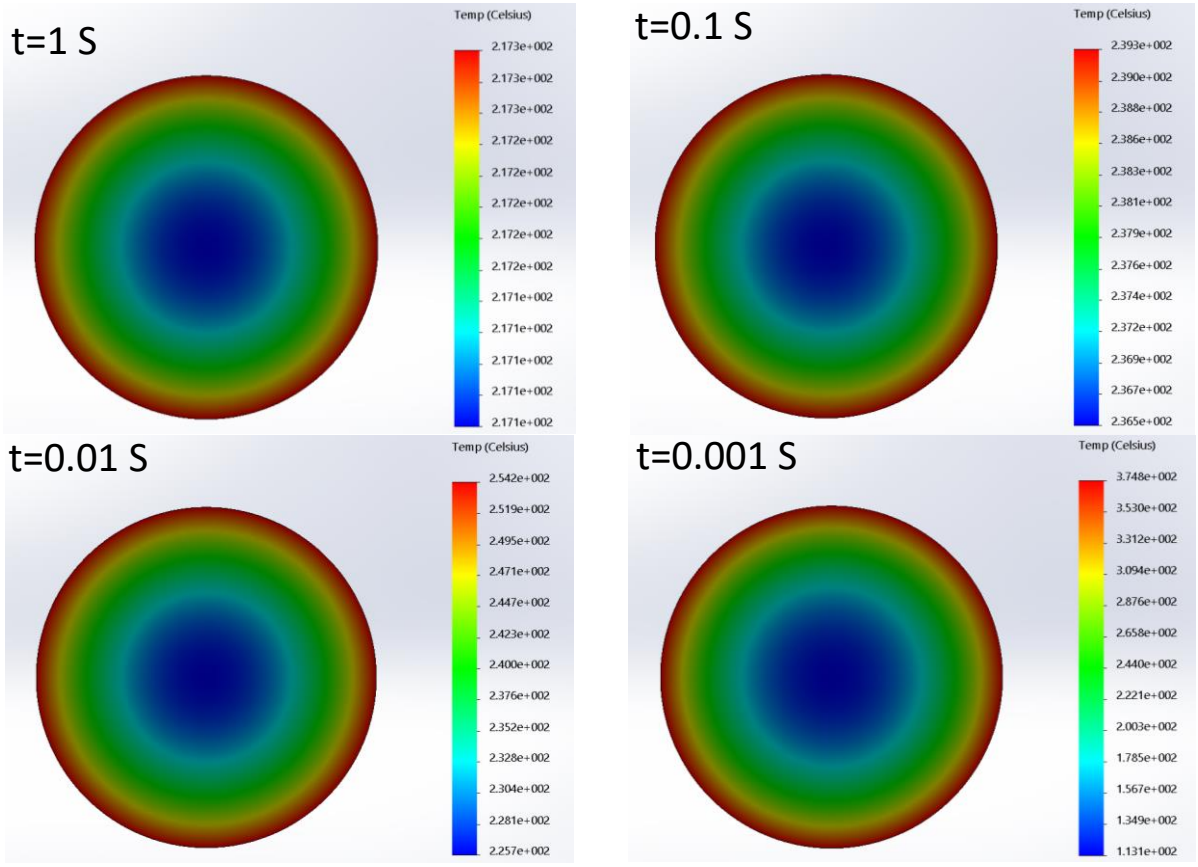

Figure 13: Temperature distribution profiles at the last time step for different pulse actuation times with the same energy input obtained by performing transient thermal finite element analysis in SolidWorks Simulation™

Table 2: Characteristics of the tested TCP muscles

Item	1-ply	2-ply
Maximum Deflection Percent	14% at 30 grams and 0.36 A.	16% at 200 grams and 0.66 A
Maximum Input Current	0.36 A at 6.5 V	0.66 A at 12 V
Maximum Input Voltage	6.5 V at 0.36 A	12 V at 0.66 A
Maximum Input Power	2.34 W	7.92 W
Maximum Input Power per length of muscle	0.11 W/cm	0.29 W/cm
Maximum Output Power*	0.0002 W	0.0023 W
Frequency tested §	0.01 Hz	0.01 Hz
Efficiency	0.03%	0.06 %

* The output power is calculated by multiplying the axial load (the hung weight) and displacement rate(velocity)
§ The frequency of silver coated TCPs can be higher ~ 7Hz when tested in water.

4. Model Calibration and Validation

The following is a comparison between the test results and the mathematical model proposed by the authors in another work. The model predicts the displacement for every weight and temperature within a certain range of validity. The specifications listed in Table 3 are used in the simulations. The model we use in this validation is taken from our previous work [35]. For the sake of brevity, only the displacement-temperature relationship in different loads are investigated, given that the temperature dynamics of the actuators are thoroughly studied in several works. The main equation of the model expressing the displacement as a function of load and temperature is reported as the following.

$$\Delta H = H_0 - \left(\frac{L_0^{\,2}}{H_0} - \frac{\pi D_0^{\,2}}{H_0} \right) \left(c_1 T + c_2 \right) \left(T - T_0 \right) + \left(\frac{D_0^{\,4}}{8 d^3 N} \frac{a T^b + E_0}{2\left(1+\mu\right)} \right)^{-1} F \tag{2}$$

Where H_0 is the coil initial length, L_0 is the precursor initial length, D_0 is the coil initial diameter, c_1 and c_2 are coefficients of the CTE changing by temperature, T is the temperature, T_0 is the initial temperature, d is the precursor diameter, a and b are the coefficients for determining the elastic modulus based on temperature. μ is the Poisson ratio, N is the number of coils, E_0 is the elastic modulus at zero temperature, and F is the axial load. The geometry of the TCP and the symbols used in the equation are depicted in Figure 14.

In Figure 15 and Figure 16, the displacement vs temperature plots are shown for 1-ply and 2-ply muscles respectively. As is shown for the most parts, the prediction accords with the experimental data. The experimental data were used for the calibration of the parameters in order to find the values for the material properties, i.e. CTE and modulus of elasticity, which were found for one set of the current and load and then applied for the whole currents and loads.

The results for 1-ply and 2-ply muscles are shown in Figure 15 and Figure 16, respectively. There are few deviations between the experimental data and model simulation. It is most visible at the results for the 2-ply muscle at low loads. As it was mentioned in the previous section, the touching of coils stops the actuator from more contraction. It can be seen in Figure 16 for the 50 and 100 grams loads. This matter is not taken into account in the proposed model as it considers the geometry of the muscles as a continuous function regardless of the boundaries. Other than this phenomenon, there is a good agreement between the simulation results and the experimental ones. One can observe it as the two curves corresponding to a certain actuation level are always close to each other.

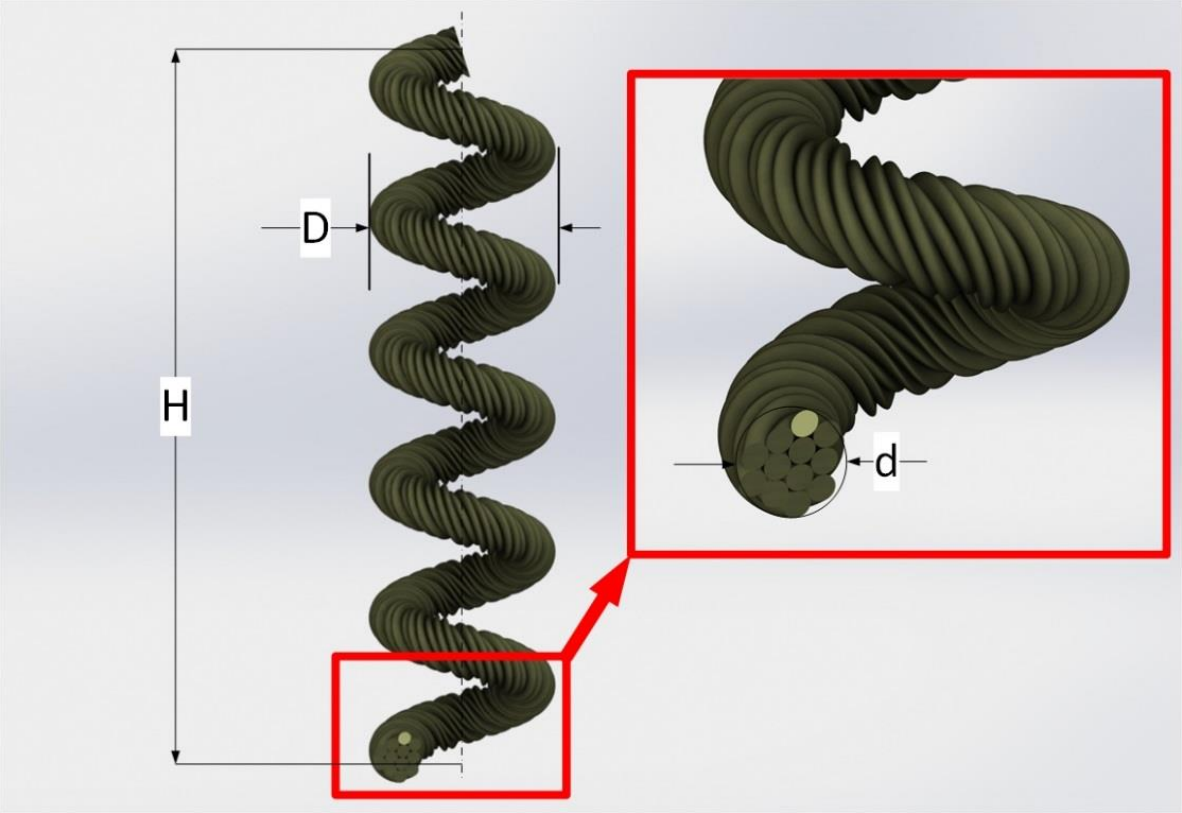

Figure 14: The geometry and notations used in the TCP muscle mathematic equation.

Table 3: Properties of the muscles used in the simulation

Parameter	Symbol	Value	Reference
Precursor Initial Length, 1-ply	$L_{0,1}$	500 mm	Measurement
Precursor Initial Length 2-ply	$L_{0,2}$	700 mm	Measurement
Coil Initial Length, 1-ply	$H_{0,1}$	150 mm	Measurement
Coil Initial Length, 2-ply	$H_{0,2}$	220 mm	Measurement
Coil Diameter	D	0.75 mm	Measurement
Initial Precursor Diameter	d_0	0.2 mm	Measurement
Stiffness in Room Temperature, 1-ply	k_1	23 N/m	Measurement
Stiffness in Room Temperature, 2-ply	k_2	26 N/m	Measurement
Ambient/Reference Temperature	T_∞	23 ºC	Measurement
First coefficient of the elastic modulus expression	a	-0.4655	Calibration
Second coefficient of the elastic modulus expression	b	1.381	Calibration
Intercept of the elastic modulus expression	E_0	536 MPa	Calibration
First coefficient of the elastic modulus expression	c_1	-3.5×10^{-6}	Calibration
Second coefficient of the elastic modulus expression	c_2	4.2×10^{-4}	Calibration

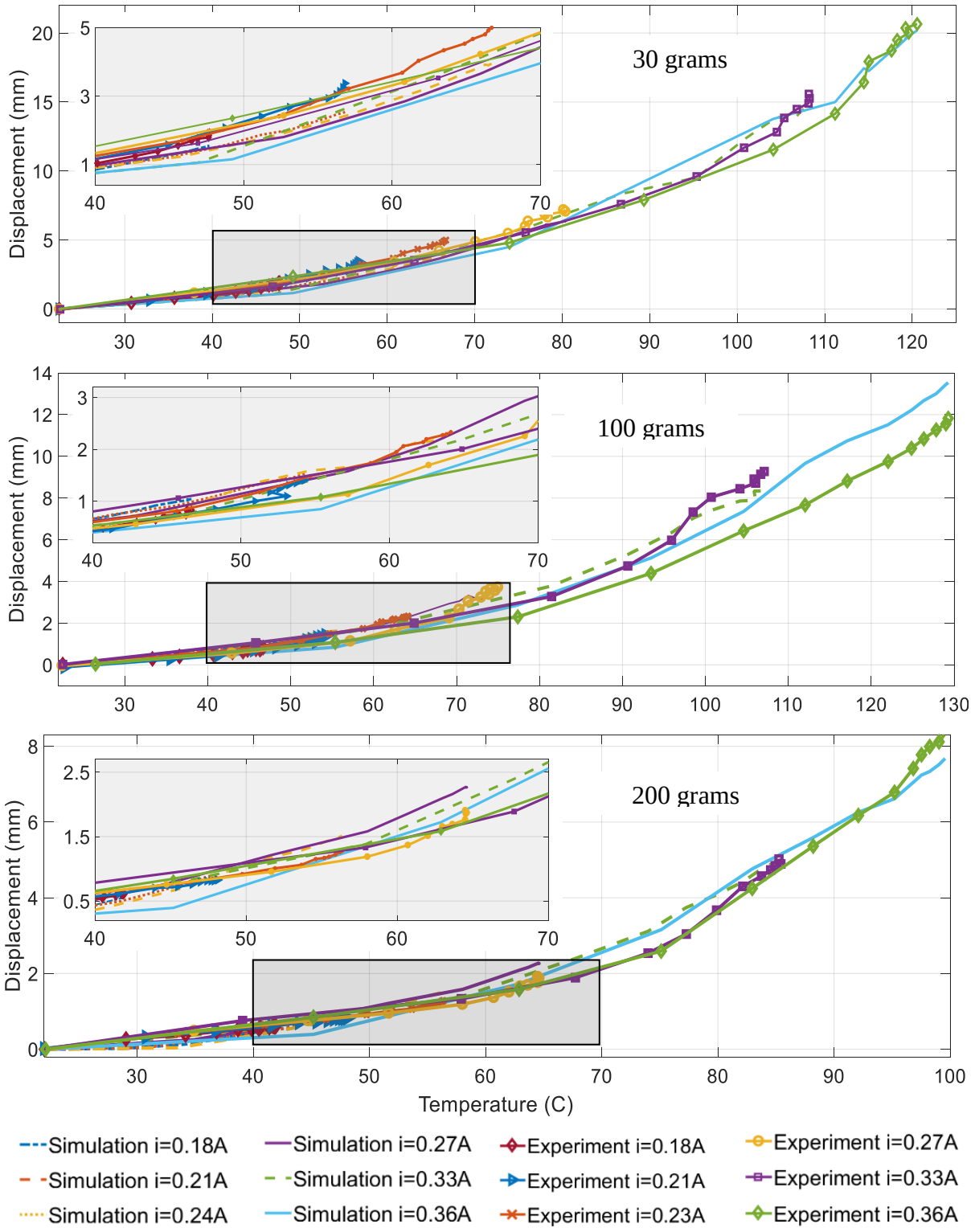

Figure 15 Displacement vs temperature of the 1-ply TCP muscle from experiment and simulation. The simulation is carried on base on the model proposed in [35]. The zoomed views are provided for a better view of the curves.

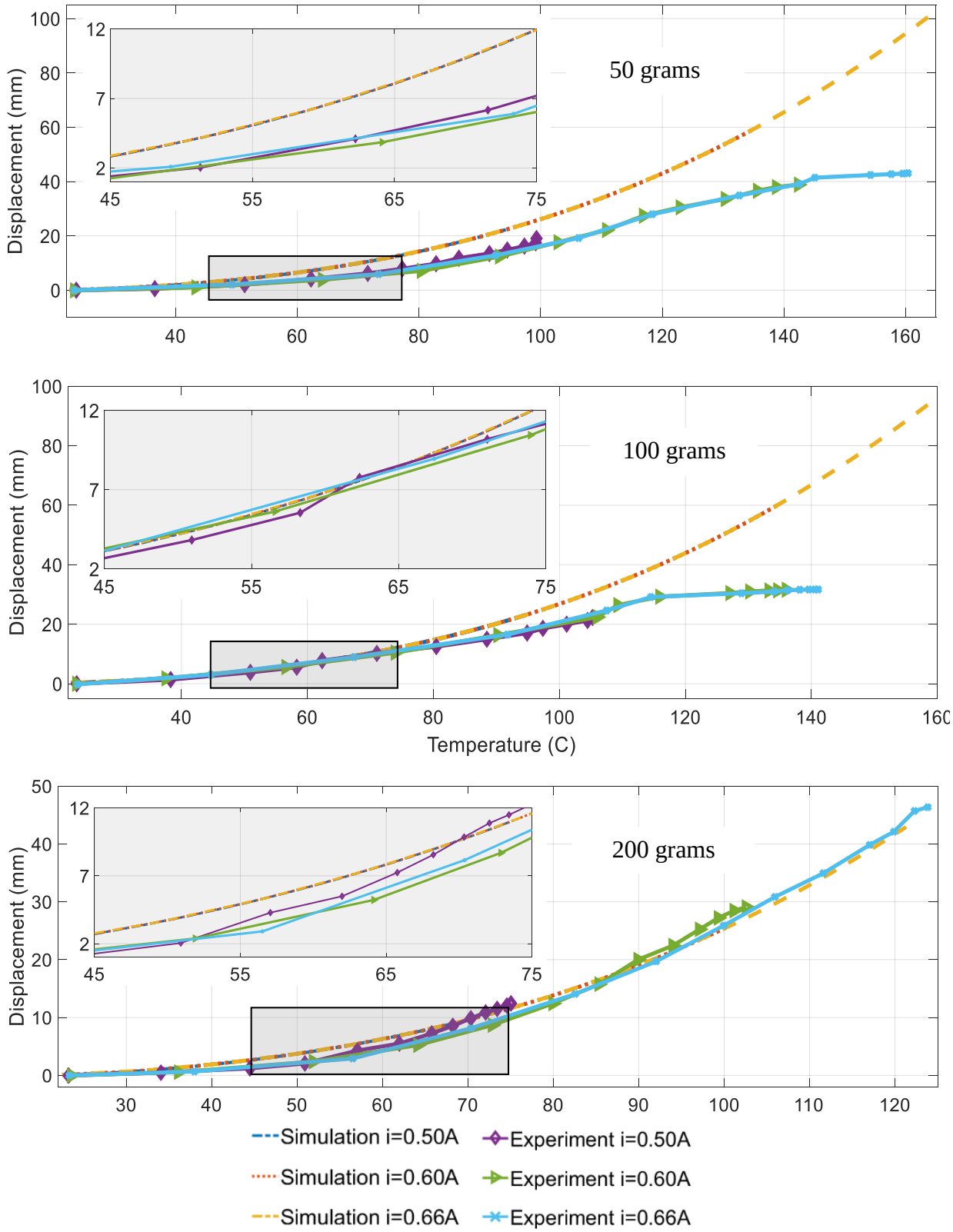

Figure 16 Displacement vs temperature of the 2-ply TCP muscle from experiment and simulation. The simulation is carried on base on the model proposed in [35]. The zoomed views are provided for a better view of the curves.

5. Conclusion, and Future Works

The aim of this study was to give an insight into the behavior and the capabilities of TCP muscles of different geometries, 1-ply and 2-ply. We demonstrated experimental data that are essential for application showing all the input and output time domain characteristics. Table 1, 2 and 3 provide the full behavior of the 1-ply and 2-ply silver coated TCP muscles, which are not reported in a comprehensive manner in many papers. We have shown fabrication parameters, actuation performance and simulation parameters. The results show that a significant actuation, as high as 16%, can be achieved by using silver-coated TCP muscles. The following observations are noticeable in the study of the results:

- The general trend in the displacement profile of the actuators shows that by increasing the load, the maximum displacement decreases when the coils in the actuators are far from contacting each other. It is an interesting topic of research for the future works. This issue is intensified after a certain load, e.g. 200 grams for the 1-ply actuator. Both the change in the geometry and also the decrease in the elastic modulus due to heating may attribute to this matter.
- The electrical resistance changes during the actuation. It can be observed by comparing the measured current and voltage as the latter increases meanwhile the former stays steady.
- The theoretical model predicted the displacement vs temperature profiles very well for 1 ply muscles, but it is less accurate for 2-ply muscles at high temperature due to its complicated shape.
- The proposed models should be used cautiously in the vicinity of the working limits, i.e. at the high or low loads or high temperature, as the nonlinear phenomena and discontinuities become more prominent. Using the models developed by making assumptions such as perfect helical geometry or having certain material properties can make a misleading in determining the actual behavior. The modeling of the actuators in their boundaries can be a future research topic.
- The maximum frequency of TCP muscle actuation without breaking due to the heat accumulation on the fibers surface is obtained through a thermal FEM analysis.

Acknowledgment

The authors would like to acknowledge the support of the Office of Naval Research (ONR), Young Investigator Program, under Grant No. N00014-15-1-2503.

References

[1] L. Hines, K. Petersen, G. Z. Lum, and M. Sitti, "Soft Actuators for Small‐Scale Robotics," *Advanced Materials,* vol. 29, p. 1603483, 2017.

[2] C. S. Haines, M. D. Lima, N. Li, G. M. Spinks, J. Foroughi, J. D. Madden*, et al.*, "Artificial muscles from fishing line and sewing thread," *Science,* vol. 343, pp. 868-872, 2014.

[3] N. R. Hollen, J. Saddler, and A. L. Langford, *Textiles*: Macmillan New York, 1968.

[4] C. S. Haines, N. Li, G. M. Spinks, A. E. Aliev, J. Di, and R. H. Baughman, "New twist on artificial muscles," *Proceedings of the National Academy of Sciences,* p. 201605273, 2016.

[5] G. M. Spinks, "Stretchable artificial muscles from coiled polymer fibers," *Journal of Materials Research,* vol. 31, pp. 2917-2927, 2016.

[6] S. M. Mirvakili, A. Rafie Ravandi, I. W. Hunter, C. S. Haines, N. Li, J. Foroughi*, et al.*, "Simple and strong: Twisted silver painted nylon artificial muscle actuated by Joule heating," 2014.

[7] L. Wu, M. Jung de Andrade, L. Saharan, , R. Rome, R. Baughman*, et al.*, "Compact and Low-cost Humanoid Hand Powered by Nylon Artificial Muscles," *Bioinspiration & Biomimetics,* vol. 12 2017.

[8] L. Saharan, M. J. d. Andrade, W. Saleem, R. H. Baughman, and Y. Tadesse, "iGrab: Hand Orthosis Powered by Twisted and Coiled Polymer Muscles," *Smart Materials and Structures,* 2017

[9] L. Wu, M. J. de Andrade, T. Brahme, Y. Tadesse, and R. H. Baughman, "A reconfigurable robot with tensegrity structure using nylon artificial muscles," in *Proc. of SPIE Vol*, 2016, pp. 97993K-1.

[10] L. Wu and Y. Tadesse, "Musculoskeletal System for Bio-Inspired Robotic Systems Based on Ball and Socket Joints," in *ASME 2016 International Mechanical Engineering Congress and Exposition*, 2016, pp. V04AT05A020-V04AT05A020.

[11] L. Wu, I. Chauhan, and Y. Tadesse, "A Novel Soft Actuator for the Musculoskeletal System," *Advanced Materials Technologies,* vol. 3, p. 1700359, 2018.

[12] Y. Almubarak and Y. Tadesse, "Twisted and coiled polymer (TCP) muscles embedded in silicone elastomer for use in soft robot," *International Journal of Intelligent Robotics and Applications,* pp. 1-17.

[13] Y. Almubarak, N. X. Maly, and Y. Tadesse, "Fully embedded actuators in elastomeric skin for use in humanoid robots," in *Electroactive Polymer Actuators and Devices (EAPAD) XX*, 2018, p. 1059416.

[14] J. van der Weijde, B. Smit, M. Fritschi, C. van de Kamp, and H. Vallery, "Self-Sensing of Displacement, Force and Temperature for Joule-Heated Twisted and Coiled Polymer Muscles via Electrical Impedance," *IEEE/ASME Transactions on Mechatronics,* 2016.

[15] A. Arjun, L. Saharan, and Y. Tadesse, "Design of a 3D printed hand prosthesis actuated by nylon 6-6 polymer based artificial muscles," in *Automation Science and Engineering (CASE), 2016 IEEE International Conference on*, 2016, pp. 910-915.

[16] K. Kim, K. H. Cho, H. S. Jung, S. Y. Yang, Y. Kim, J. H. Park*, et al.*, "Double Helix Twisted and Coiled Soft Actuator from Spandex and Nylon," *Advanced Engineering Materials,* 2018.

[17] S. H. Kim, M. D. Lima, M. E. Kozlov, C. S. Haines, G. M. Spinks, S. Aziz*, et al.*, "Harvesting temperature fluctuations as electrical energy using torsional and tensile polymer muscles," *Energy & Environmental Science,* vol. 8, pp. 3336-3344, 2015.

[18] B. Pawlowski, J. Sun, J. Xu, Y. Liu, and J. Zhao, "Modeling of Soft Robots Actuated by Twisted-and-Coiled Actuators," *IEEE/ASME Transactions on Mechatronics,* 2018.

[19] S. Mendes and L. Nunes, "Experimental approach to investigate the constrained recovery behavior of coiled monofilament polymer fibers," *Smart Materials and Structures,* vol. 26, p. 115031, 2017.

[20] A. Cherubini, G. Moretti, R. Vertechy, and M. Fontana, "Experimental characterization of thermally-activated artificial muscles based on coiled nylon fishing lines," *AIP Advances,* vol. 5, p. 067158, 2015.

[21] D. Yue, X. Zhang, H. Yong, J. Zhou, and Y.-H. Zhou, "Controllable rectification of the axial expansion in the thermally driven artificial muscle," *Applied Physics Letters,* vol. 107, p. 111903, 2015.

[22] D. Yue, X. Zhang, J. Zhou, and Y.-H. Zhou, "Effective Young's modulus of the artificial muscle twisted by fishing lines: Analysis and experiment," *AIP Advances,* vol. 5, p. 097113, 2015.

[23] T. Li, Y. Wang, K. Liu, H. Liu, J. Zhang, X. Sheng*, et al.*, "Thermal actuation performance modification of coiled artificial muscle by controlling annealing stress," *Journal of Polymer Science Part B: Polymer Physics,* vol. 56, pp. 383-390, 2018.

[24] A. M. Swartz, D. R. Ruiz, H. Feigenbaum, M. Shafer, and C. C. Browder, "Experimental characterization and model predictions for twisted polymer actuators in free torsion," *Smart Materials and Structures,* 2018.

[25] S. Sharafi and G. Li, "A multiscale approach for modeling actuation response of polymeric artificial muscles," *Soft matter,* vol. 11, pp. 3833-3843, 2015.
[26] Q. Yang and G. Li, "A top-down multi-scale modeling for actuation response of polymeric artificial muscles," *Journal of the Mechanics and Physics of Solids,* vol. 92, pp. 237-259, 2016.
[27] M. Jafarzadeh, L. Wu, and Y. Tadesse, "System Identification of Force of a Silver Coated Twisted And Coiled Polymer Muscle," in *IMECE 2017*, Tampa , Florida, 2017.
[28] M. Jafarzadeh, N. Gans, and Y. Tadesse, "Control of TCP muscles using Takagi–Sugeno–Kang fuzzy inference system," *Mechatronics,* vol. 53, pp. 124-139, 8// 2018.
[29] T. Arakawa, K. Takagi, K. Tahara, and K. Asaka, "Position control of fishing line artificial muscles (coiled polymer actuators) from nylon thread," in *SPIE Smart Structures and Materials+ Nondestructive Evaluation and Health Monitoring*, 2016, pp. 97982W-97982W-12.
[30] A. Abbas and J. Zhao, "A physics based model for twisted and coiled actuator," in *Robotics and Automation (ICRA), 2017 IEEE International Conference on*, 2017, pp. 6121-6126.
[31] M. C. Yip and G. Niemeyer, "On the Control and Properties of Supercoiled Polymer Artificial Muscles," *IEEE Transactions on Robotics,* 2017.
[32] J. Zhang, K. Iyer, A. Simeonov, and M. C. Yip, "Modeling and Inverse Compensation of Hysteresis in Supercoiled Polymer Artificial Muscles," *IEEE Robotics and Automation Letters,* vol. 2, pp. 773-780, 2017.
[33] J. Zhang, A. Simeonov, and M. C. Yip, "Three-dimensional Hysteresis Compensation Enhances Accuracy of Robotic Artificial Muscles," *Smart Materials and Structures,* 2018.
[34] K. Masuya, S. Ono, K. Takagi, and K. Tahara, "Modeling framework for macroscopic dynamics of twisted and coiled polymer actuator driven by Joule heating focusing on energy and convective heat transfer," *Sensors and Actuators A: Physical,* vol. 267, pp. 443-454, 2017.
[35] F. Karami and Y. Tadesse, "Modeling of twisted and coiled polymer (TCP) muscle based on phenomenological approach," *Smart Materials and Structures,* vol. 26, p. 125010, 2017.
[36] S. Aziz, S. Naficy, J. Foroughi, H. R. Brown, and G. M. Spinks, "Twist–Coil Coupling Fibres for High Stroke Tensile Artificial Muscles," *Sensors and Actuators A: Physical,* 2018.
[37] L. Wu and Y. Tadesse, "Modeling of the Electrical Resistance of TCP Muscle," in *IMECE 2017*, Tampa , Florida, 2017.